

Densification and Mechanical Properties of Electroconductive Si_3N_4 -Based Composites Prepared by Spark Plasma Sintering

(Penumpatan dan Sifat-Sifat Mekanik Komposit Berasaskan Si_3N_4 disediakan Melalui Pensinteran Percikan Plasma)

NORHAYATI AHMAD* & HIDEKAZU SUEYOSHI

ABSTRACT

Si_3N_4 -TiN composites were prepared by conventional powder processing (SPS1) and in-situ reaction sintering (SPS2). Rapid densification of SPS was achieved for sample SPS1 and SPS2 within a few minutes at low temperature. Sample SPS1 sintered at 1550°C showed rapid transformation of α to β Si_3N_4 while for sample SPS2 sintered at 1350°C, a significant degree of α to β Si_3N_4 transformation was achieved. Homogeneous distribution of equiaxed TiN grains in matrix Si_3N_4 resulting in high hardness (21.7 GPa) and bending strength (621 MPa) for sample SPS1 sintered at 1550°C. Elongated TiN grains as the reinforcement of Si_3N_4 matrix composites was found to increase the toughness (8.39 MPa $\text{m}^{1/2}$) of sample SPS2 sintered at 1350°C. The composites prepared by SPS2 sintered at 1250-1350°C had low electrical resistivity and could be machined by electrical discharge machining (EDM).

Keywords: Densification; mechanical properties; silicon nitride-titanium nitride composites; spark plasma sintering

ABSTRAK

Komposit Si_3N_4 -TiN dihasilkan dengan kaedah pemprosesan serbuk yang lazim (SPS1) dan pensinteran tindak balas in-situ (SPS2). Pemandatan yang tinggi diperolehi daripada sampel SPS1 dan SPS2 selama beberapa minit pada suhu yang rendah. Sampel SPS1 yang disinter pada suhu 1550°C menunjukkan transformasi daripada α ke β Si_3N_4 yang pantas manakala sampel SPS2 yang disinter pada suhu 1350°C menunjukkan transformasi α ke β Si_3N_4 ke tahap yang signifikan. Taburan butiran TiN yang berbentuk sepaksi secara seragam dalam matrik Si_3N_4 memberikan kekerasan (21.7 GPa) dan kekuatan lenturan (621 MPa) yang tinggi bagi sampel SPS1 yang disinter pada suhu 1550°C. Butiran TiN yang berbentuk panjang sebagai penguat dalam matrik komposit Si_3N_4 boleh meningkatkan ketahanan (8.39 MPa $\text{m}^{1/2}$) bagi sampel SPS2 yang disinter pada suhu 1350°C. Sampel SPS2 yang disinter pada suhu 1250-1350°C mempunyai rintangan elektrik yang rendah dan boleh dimesin dengan pemesinan nyahcas elektrik (EDM).

Kata kunci: Komposit silikon nitrat-titanium nitrat; pensinteran percikan plasma (SPS); penumpatan; sifat mekanikal

INTRODUCTION

Si_3N_4 -based ceramics are promising materials for applications in gas turbine components, heat exchangers and wear-resistant components. Most of these applications require good strength and toughness, high thermal conductivity and good environmental stability at high temperature. Furthermore, Si_3N_4 components must be machined by using diamond tool, due to their low electrical conductivity. Diamond machining is a costly process, which also implies limitations on the complexity of the final shapes. The addition of electroconductive phases to insulating ceramics in suitable amounts is a straightforward strategy to overcome this problem, since it allows components to be machined by electro-discharge machining (EDM) (Bellosi et al. 1992; Liu & Huang 2003). All these considerations have led to the attempt to fabricate electroconductive Si_3N_4 -based materials with improved mechanical properties. For this aim, the Si_3N_4 matrix was simultaneously added with TiN particles. TiN has been coupled to several ceramic matrixes, such as Si_3N_4 , Al_2O_3 , ZrO_2 and it has been found that TiN addition causes a

significant improvement in the mechanical properties (Bellosi et al. 1992; Liu & Huang 2003; Salehi et al. 2006; Wang et al. 2006) and the oxidation resistance (Mazerolles et al. 2005).

Recent development of novel sintering techniques enables us not only to produce dense solids, but also to control their microstructure and mechanical properties. Spark plasma sintering (SPS) is similar to hot-pressing to the extent that graphite dies are used, but the heating is accomplished by spark discharges in voids between the particles, generated by an instantaneous pulsed direct current which is applied through electrodes at the top and bottom punches of the graphite die. Due to these discharges, the particle surface is activated and purified, and a self-heating phenomenon is generated between the particles, as a result of which heat-transfer and mass-transfer can be completed instantaneously (Gao & Miyamoto 1997; Gao et al. 1998; Parera et al. 1998; Tokita 1993). Many investigations have been performed concerning the densification mechanism of Si_3N_4 -based ceramics by rapid sintering process. It is said that the sintering

proceeds very quickly mainly because of the spark plasma caused by the large pulse current, thus allowing nanosized grains of the starting powder and its crystal structure as well, to be retained in the sintered body. Generally, the Kingery sintering model has been used in describing the densification results (Bowen et al. 1978; Lewis 1980; Messier et al. 1978). Today, most Si_3N_4 ceramics are prepared by using α -rich Si_3N_4 powders, which transform during sintering into β - Si_3N_4 . The β -modification forms elongated needle-like grains with high aspect ratios. This can be attributed to the relatively complex microstructure developed during densification by liquid phase sintering (Weiss & Kaysser 1978)

The objective of this work was to compare the sinterability, the microstructure and the mechanical properties of Si_3N_4 – TiN composites prepared by conventional sintering of a mixture of Si_3N_4 and TiN powders and *in-situ* reaction sintering of Si_3N_4 and Ti powders. By using a novel rapid sintering method, SPS has been applied to sinter a composite at different temperatures. The samples obtained by SPS have advantages such as a more homogeneous microstructure, a higher density and excellent mechanical properties.

EXPERIMENTAL METHODS

The basic raw material used for preparing the composites was nanosized Si_3N_4 powder containing 5 mass % Y_2O_3 and 2 mass % Al_2O_3 as sintering additive (Wako Co. Ltd., mean particle size 60 nm). The Si_3N_4 powder was mixed with TiN powder (Wako Co. Ltd., mean particle size 50 nm) and Ti powder (Wako Co. Ltd., mean particle size 45 μm) for sample SPS1 and SPS2, respectively. The composition of starting powder mixtures and some details about preparation methods used in experiments are shown in Table 1.

The powders measured according to Table 1 were mixed by planetary ball milling (Pulverisette 6, Fritsch Co. Ltd.) in ethanol. After drying, the mixed powders were screened and enclosed in a graphite die, then were sintered by SPS-3.20 MK-4 (Sumitomo Coal Co. Ltd.). During heating, the change in thickness of the specimen was measured by a dilatometer to monitor the densification behaviour. Sintered disks obtained by SPS were 15 mm in diameter. Density measurements were

made using the Archimedes technique with an immersion medium of distilled water. The crystalline structure was examined by X-ray diffraction (XRD-6000S, Shimadzu Co. Ltd.), which was performed with CuK_α radiation at a scanning rate of $3^\circ/\text{min}$. By comparing the peak intensity in the XRD patterns, the α/β - Si_3N_4 ratios were calculated based on measurements of the ratio of intensities of the α_{201} and β_{201} reflections (Kall 1988). All the resulting disks were cut and ground into bars ($3 \times 4 \times 15 \text{ mm}^3$) for strength measurements. The strength was measured with a mechanical machine (AG-1, Shimadzu Co. Ltd.) using three-point bending test with a span length of 10 mm and a crosshead speed of 0.1 mm/min. Fracture surfaces were examined by scanning electron microscopy (ESEM XL-30 Series, Philips Co. Ltd.). Hardness was obtained by Vickers microhardness (HMV, Shimadzu Co. Ltd.) with an indentation load of 19.614 N for 30 s. The fracture toughness was measured by indentation method and calculated according to the equation given by Niihara et.al. (1982). The electrical resistivity was measured at room temperature on the polished surface of the specimen ($2 \times 3 \times 14 \text{ mm}^3$) using the four-point probe method. The machinability of the composites was examined by EDM (Robocut α -OA, Fanuc Co. Ltd.) with 0.25 mm diameter of Cu wire at a speed of 0.2 mm/min.

RESULTS AND DISCUSSION

Typical shrinkage data ($\Delta L/L_0$) recorded during sintering of SPS1 and SPS2 versus time are shown in Figures 1 and 2, respectively. The shrinkage curves recorded for sample SPS1 sintered at 1550 and 1600°C showed a narrow time interval ranging from ~18 min to ~23.5 min which densify in a very short time (~5.5 min) compared with sample sintered at 1450 and 1500°C (~11 min). Sample SPS2 sintered at 1300 and 1350°C showed rapid densifications (~8.5 min) as compared with sample sintered at 1200 and 1250°C (~11 min). Rapid densification of SPS was achieved for sample SPS1 and SPS2 within a few minutes. In conventional hot pressing, the densification of Si_3N_4 -based ceramics takes several hours and the densification is accompanied by phase transformations/reactions and grain growth. Using SPS, however, the densification of Si_3N_4 -TiN composites can be accomplished by sintering for short holding time at low temperature.

TABLE 1. Starting compositions and preparation conditions of Si_3N_4 -TiN composites

Samples	Starting powders (mass %)			Ball milling parameter		Sintering parameter			
	Si_3N_4	TiN	Ti	Time (h)	Speed (rpm)	Temperature (°C)	Heating rate (°C/min)	Pressure (MPa)	Holding time (min)
SPS1	70	30	-	6	100	1450-1600	100	40	10
SPS2	70	-	30	30	200	1200-1450	100	40	10

TABLE 2. Density (ρ), crystalline phase (β -Si₃N₄), Vickers microhardness (Hv), bending strength (σ), fracture toughness (K_{1C}) and electrical resistivity of composites at different temperatures

Samples	T (°C)	ρ (g/cm ³)	β -Si ₃ N ₄ (%)	H _v (GPa)	σ (MPa)	K _{1C} (MPa m ^{1/2})	Electrical resistivity (Ω cm)
SPS1	1450	3.13	66.6	7.61	183	2.67	5x10 ¹³
	1500	3.47	87.7	19.53	547	3.10	8.73 × 10 ⁴
	1550	3.65	90.8	21.71	621	4.16	6.14 × 10 ²
	1600	3.65	91.6	18.99	569	3.36	3.46
SPS2	1200	2.69	47.1	5.48	155	1.72	1.24
	1250	3.03	49.2	7.56	198	3.24	6.30 × 10 ⁻²
	1300	3.24	51.5	17.78	355	8.39	1.33 × 10 ⁻¹
	1350	3.41	58.5	19.95	328	6.56	4.29 × 10 ⁻¹
	1450	3.30	98.3	17.96	292	4.64	1.82 × 10 ²
	1550	3.29	100.0	17.34	262	4.39	1.40 × 10 ³

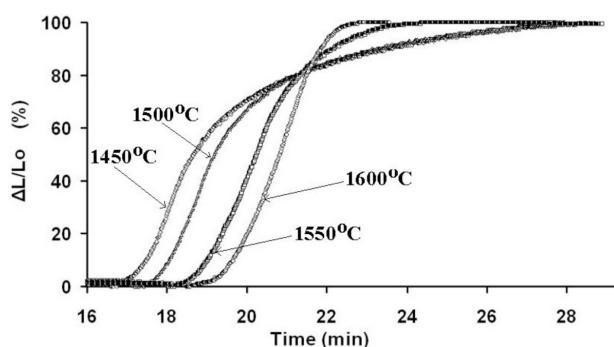


FIGURE 1. Shrinkage ($\Delta L/L_0$) curves recorded with sintering time for sample SPS1

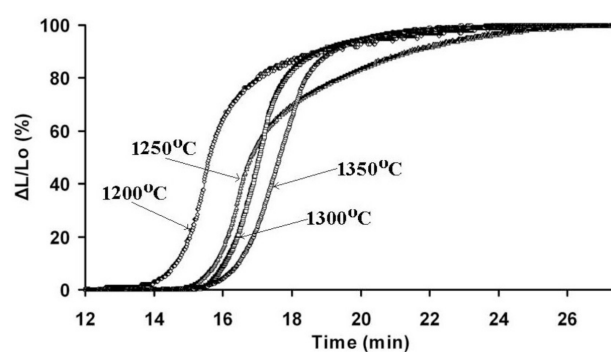


FIGURE 2. Shrinkage ($\Delta L/L_0$) curves recorded with sintering time for sample SPS2

As discussed in previous work (Norhayati Ahmad et al. 2009) the logarithm of shrinkage ($\ln \Delta L/L_0$) was plotted versus logarithm of isothermal holding time ($\ln t$) in order to determine the densification mechanism at early stage of sintering. The dominant mechanisms of sample SPS1 at 1450 and 1500°C were a hybrid of dissolution-precipitation and viscous flow and at 1600°C, the dominant mechanism was viscous flow. The dissolution of precipitate Si₃N₄ grains at early-formed oxygen-rich liquid is restricted below a certain critical temperature (1500°C) and above this temperature, e.g 1600°C, the viscous flow is the dominant mechanisms because the dissolution process takes place rapidly and large amount of nitrogen-containing liquid is formed. The dominant mechanism for sample SPS2 at 1200 - 1300°C was a hybrid of dissolution-precipitation and viscous flow (Norhayati Ahmad & Sueyoshi 2010, 2011). The synthesis of TiN by reaction sintering was promoted by dissolution-precipitation and viscous flow during SPS. The precipitate of small nodular β -Si₃N₄ initiated the solution of Si₃N₄ at contact point between particles and transported from small to large grain by diffusion. This nodular reacted with TiO₂

(from the surface of Ti powder) and Ti to form TiN. The large TiN grains grow at the expense of the small β -Si₃N₄ during the liquid-phase sintering. The formation of TiN along the nodular β -Si₃N₄ could be densified more quickly because of the rapid sintering rate in SPS.

β -Si₃N₄ content at different temperatures for sample SPS1 and SPS2 is shown in Table 2. The formation of β -Si₃N₄ is almost completed (90.8%) at 1550°C for sample SPS1, while the transformation from α to β -Si₃N₄ is not completed (58.5%) at 1350°C for sample SPS2. Therefore, for sample SPS1, the phase transformation happens and almost completes at a lower temperature with almost β -Si₃N₄ could be obtained at higher sintering temperature. On the other hand, a small degree of phase transformation of sample SPS2 occurs at lower temperature. Afterwards, sintering at higher temperature will cause further phase transformation that leads to rapid grain growth. Phase transformation and synthesis of Si₃N₄-based composite of sample SPS2 at lower temperature compared with sample SPS1 because liquid phase may spread around the Si₃N₄ particles due to pressure.

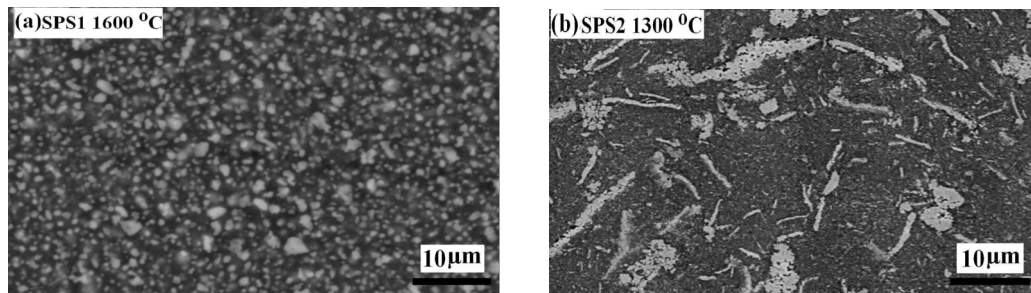


FIGURE 3. BSE images of polished surfaces for sample (a) SPS 1 and (b) SPS 2

The BSE images of sample SPS1 sintered at 1600°C and SPS2 sintered at 1300°C are shown in Figure 3. The grey and white contrast phases are respectively the Si_3N_4 and TiN phase which was identified by EDX analysis. A homogeneous distribution of TiN particles was achieved by SPS1 at 1600°C (Figure 3(a)). Elongated TiN grains observed in sample SPS2 (Figure 3(b)) clearly indicates the formation of in-situ TiN grains during sintering.

The formations of equiaxed TiN grains for sample SPS1 are uniformly distributed in the Si_3N_4 matrix which contained fine-grained $\beta\text{-Si}_3\text{N}_4$ phase which resulted in high strength and hardness (Table 2). The nucleation and growth of TiN and silicon nitride grains occurred at the same time in this composite. For sample SPS2, the phase transformation and grain growth progresses so fast to develop into microstructures consisting of elongated TiN needles reinforced in the fine grains matrix Si_3N_4 with improved fracture toughness (Table 2). However, the presence of too large elongated TiN grains at higher temperature will deteriorated the fracture toughness. As shown in Table 2, the electrical resistivity of sample SPS2 sintered at 1250 - 1350°C ($6.30 \times 10^{-2} - 4.29 \times 10^{-1} \Omega \text{ cm}$) are enough to be EDM is machinable. This can be explained by the increased connectivity of elongated TiN grains in sample SPS2 as shown in Figure 3(b).

CONCLUSION

Almost all $\alpha\text{-Si}_3\text{N}_4$ transform to $\beta\text{-Si}_3\text{N}_4$ for sample SPS1 sintered at 1550°C. For sample SPS2 sintered at 1300°C the reaction can be accomplished with very limited involvement of phase transformation. Therefore, the phase transformation sequence can be precisely followed and manipulated during further annealing after complete densification. The use of local thermal difference generated by the SPS under rapid heating and a short holding time appears to be a very effective way for producing well dispersed equiaxed TiN (sample SPS1) and elongated TiN (SPS2) which has been suggested to enhance the mechanical and electrical properties.

ACKNOWLEDGEMENT

We thank Dr. Y. Kawakami from Ind. Tech. Center of Saga, Japan for the SPS apparatus.

REFERENCES

- Bellosi, A., Guicciardi, S. & Tampieri, A. 1992. Development and characterization of electroconductive $\text{Si}_3\text{N}_4\text{-TiN}$ composites *J. Eur. Ceram. Soc.* 9: 83-93.
- Bowen, L.J., Carruthers, T.G. & Brook, R.J. 1978. Hot-pressing of silicon nitride with yttrium oxide and lithium oxide as additives: *J. of the Am. Cer. Soc.* 61: 335-339.
- Bowen, L.J., Weston, R.J., Carruthers, T.G. & Brook, R.J. 1978. Hot-pressing and the $\alpha\text{-}\beta$ phase transformation in silicon nitride. *J. of Mat. Sc.* 13: 341-350.
- Gao, L., Hong, J.S., Miyamoto, H. & Torre, S.D.D.L. 1998. Superfast densification of oxide ceramics by spark plasma sintering. *J. Inorg. Mater.* 13: 18-22.
- Gao, L. & Miyamoto, H. 1997. Spark Plasma Sintering Technology. *J. Inorg. Mater.* 12: 129-133.
- Kall, P.O. 1988. Quantitative phase analysis of Si_3N_4 -based Materials *Chem. Scr.* 28: 439-4368.
- Lewis, M.H., Bhatti, A.R., Lumby, R.J. & North, B. 1980. The microstructure of sintered Si-Al-O-N ceramics, *J. of Mat. Sc.* 15: 103-113.
- Liu, C.C. & Huang, J.L. 2003. Effect of the electrical discharge machining on strength and reliability of $\text{TiN/Si}_3\text{N}_4$ composites. *Ceram. Inter* 29: 679-687.
- Mazerolles, L., Feldhoff, A., Trichet, M. F. & Ricoult, M.B. 2005. Oxidation behaviour of $\text{Si}_3\text{N}_4\text{-TiN}$ ceramics under dry and humid air at high temperature. *J. of the Eur. Ceram. Soc* 25: 1743-1748.
- Messier, D.R., Riley, F.L. & Brook, R. J. 1978. The α/β silicon nitride phase transformation, *J. of Mat. Sc.* 13: 1199-1205.
- Niihara, K., Morena, R. & Hasselman, D.P.H. 1982, Evaluation of K_{IC} of brittle solids by the indentation method with low crack-to-indent ratios. *J. Mater Sc. Letter* 1: 13-16.
- Norhayati Ahmad, Obara, K., Sameshima, S. & Sueyoshi, H. 2009. Characterization of $\text{Si}_3\text{N}_4\text{-TiN}$ composites prepared by spark plasma sintering, *trans. Mater. Res. Soc. Japan* 32(4): 793-797.
- Norhayati Ahmad & Sueyoshi, H. 2010. Properties of $\text{Si}_3\text{N}_4\text{-TiN}$ Composites Fabricated by Spark Plasma Sintering by Using a Mixture of Si_3N_4 and Ti Powders. *Ceram. Int.* 36: 491-496.
- Norhayati Ahmad & Sueyoshi, H. 2011. Microstructure and mechanical properties of silicon nitride-titanium nitride composites prepared by spark plasma sintering. *Materials Research Bulletin* 46: 460-63.
- Perera, D.S., Tokita, M. & Moricca, S. 1998. Comparative study of fabrication of $\text{Si}_3\text{N}_4/\text{SiC}$ composites by spark plasma sintering and hot isostatic pressing. *J. Eur. Ceram. Soc.* 18: 401-404.

- Salehi, S., Biest, O.V. & Vleugels, J. 2006. Electrically conductive ZrO₂-TiN composites. *J. of the Eur. Ceram. Soc.* 26. 3173-3179.
- Tokita, M. 1993. Mechanism of spark plasma sintering. *J. Soc. Powder Tech. Jpn.* 30(11): 790-804.
- Wang, L., Wu, T., Jiang, W., Li, J. & Chen, L. 2006. Consolidation of nano-sized TiN powders by spark plasma sintering. *J. Am. Ceram. Soc.* 89(5): 1540-1543.
- Weiss, J. & Kaysser, W.A. 1983. Liquid phase sintering in. In: (ed.), *Progress in Nitrogen Ceramics*, F.L. Riley (ed.) Boston: Martinus Nijhoff Publishers pp. 169.

Hidekazu Sueyoshi
Department of Nano-structure and Advanced Materials
Graduate School of Science and Engineering
Kagoshima University, 1-21-40 Korimoto
Kagoshima 890-0065 Japan

*Corresponding author; email: nhayati@fkm.utm.my

Received: 25 January 2010

Accepted: 25 March 2011

Norhayati Ahmad*
Department of Materials Engineering
Faculty of Mechanical Engineering
Universiti Teknologi Malaysia
81310 UTM Skudai
Johor, Malaysia